

The decay constants f_B and f_{D^+} from three-flavor lattice QCD

C. Bernard^a, C. DeTar^b, M. Di Pierro^c, A.X. El-Khadra^d, R.T. Evans^d, E. Freeland^{e,i}, E. Gamiz^d, Steven Gottlieb^f, U.M. Heller^g, J.E. Hetrick^h, R. Jain^d, A.S. Kronfeldⁱ, J. Laiho^{ia}, L. Levkova^b, P.B. Mackenzieⁱ, D. Renner^j, J.N. Simone^{*i}, R. Sugar^k, D. Toussaint^j, and R.S. Van de Waterⁱ

^aDepartment of Physics, Washington University, St. Louis, Missouri, USA

^bPhysics Department, University of Utah, Salt Lake City, Utah, USA

^cSchool of Computer Sci., Telecom. and Info. Systems, DePaul University, Chicago, Illinois, USA

^dPhysics Department, University of Illinois, Urbana, Illinois, USA

^eLiberal Arts Department, The School of the Art Institute of Chicago, Chicago, Illinois, USA

^fDepartment of Physics, Indiana University, Bloomington, Indiana, USA

^gAmerican Physical Society, One Research Road, Box 9000, Ridge, New York, USA

^hPhysics Department, University of the Pacific, Stockton, California, USA

ⁱFermi National Accelerator Laboratory, Batavia, Illinois, USA

^jDepartment of Physics, University of Arizona, Tucson, Arizona, USA

^kDepartment of Physics, University of California, Santa Barbara, California, USA

E-mail: simone@fnal.gov

Fermilab Lattice and MILC Collaborations

We present new preliminary results for the leptonic decay constants f_B and f_{D^+} determined in $2+1$ flavor lattice QCD at lattice spacings $a = 0.09, 0.12$ and 0.15 fm. Results are obtained using the MILC Collaboration gauge configuration ensembles, clover heavy quarks in the Fermilab interpretation and improved staggered light quarks. Decay constants, computed at partially quenched combinations of the valence and sea light quark masses, are used to determine the low-energy parameters of staggered chiral perturbation theory. The physical decay constants are found in an extrapolation using the parameterized chiral formula.

The XXV International Symposium on Lattice Field Theory
July 30-4 August 2007
Regensburg, Germany

*Speaker.

1. Introduction

The D meson decay constants, when compared to precise experimental results, are a critical check of the lattice methods needed for f_B . In Ref. [1] we predicted $f_{D^+} = 201 \pm 3 \pm 17$ MeV in good agreement with the CLEO-c measurement $f_{D^+} = 223 \pm 17 \pm 3$ MeV revealed days later [2].

In this work we present new results for the D and B meson decay constants. Precise determinations of f_B , f_{B_s} and the ratio f_{B_s}/f_B are needed to study the Standard Model picture of B - \bar{B} and B_s - \bar{B}_s mixing. A progress report for the mixing matrix element study is presented in Ref. [3].

2. Simulation details

We use the MILC Collaboration three-flavor asqtad ensembles [4]. Details are tabulated in Table 1. For these ensembles, m_l denotes the mass of the two degenerate lighter sea quarks. A single heavier sea quark has a mass m_h near the strange quark mass. Upsilon spectroscopy tells us the heavy quark potential scale $r_1 = 0.318(7)$ fm [5]. The number of valence quark masses, $\#m_q$, used in this study is listed in the last column of the table.

The leptonic decay constant f_{H_q} for a meson H_q is defined by

$$\langle 0 | A_\mu | H_q(p) \rangle = i f_{H_q} p_\mu . \quad (2.1)$$

The combination $\phi_{H_q} = f_{H_q} \sqrt{m_{H_q}}$ emerges from a combined fit to lattice 2-pt functions:

$$C_O(t) = \langle O_{H_q}^\dagger(t) O_{H_q}(0) \rangle \quad (2.2)$$

$$C_{A_4}(t) = \langle A_4(t) O_{H_q}(0) \rangle , \quad (2.3)$$

where O_{H_q} can be either a smeared or local operator.

The axial current renormalization is taken to be

$$Z_{A_4}^{Qq} = \rho_{A_4}^{Qq} \sqrt{Z_{V_4}^{QQ} Z_{V_4}^{qq}} . \quad (2.4)$$

a [fm]	am_h	am_l	β	r_1/a	configs	$\# m_q$
0.09	0.031	0.0031	7.08	3.69	435	11
		0.0062	7.09	3.70	557	10
		0.0124	7.11	3.72	518	8
0.12	0.05	0.005	6.76	2.64	529	12
		0.007	6.76	2.63	833	12
		0.01	6.76	2.62	592	12
		0.02	6.79	2.65	460	12
		0.03	6.81	2.66	549	12
0.15	0.0484	0.0097	6.572	2.13	631	9
		0.0194	6.586	2.13	631	9
		0.029	6.600	2.13	440	9

Table 1: MILC three-flavor lattice parameters. The last column lists the number of valence light quarks used in this study.

Factors $Z_{V_4}^{ff}$ are fixed nonperturbatively from scattering 3-pt functions and the known normalization of the vector current. Factors $\rho_{A_4}^{Qq}$ are known to one-loop order and are close to unity [6].

3. Staggered Chiral Perturbation Theory (S χ PT)

With staggered quarks the (squared) taste-nonsinglet pseudoscalar meson masses are split:

$$M_{ab,\xi}^2 = (m_a + m_b)\mu + a^2\Delta_\xi, \quad (3.1)$$

where m_a, m_b are quark masses and the (sixteen) mesons are labeled by their taste representation $\xi = P, A, T, V, I$ with $\Delta_P = 0$.

At next-to-leading order (NLO) in χ PT the expression for the decay constants is

$$\phi_{H_q} = \Phi_H [1 + \Delta f_H(m_q, m_l, m_h) + p_H(m_q, m_l, m_h)] \quad (3.2)$$

where Δf_H denotes the ‘‘chiral logs’’ and p_H denotes terms analytic in the meson masses.

With staggered quarks

$$\Delta f_H = -\frac{1 + 3g_{H^*H\pi}^2}{2(4\pi f_\pi)^2} [\bar{h}_q + h_q^I + a^2 (\delta'_A h_q^A + \delta'_V h_q^V)]. \quad (3.3)$$

Taste-breaking effects arise at finite a from the meson mass splittings and the δ'_A and δ'_V hair-pin terms [7]. Finite a effects reduce the chiral logarithm curvature, however, the expected QCD chiral logarithm is recovered in the continuum limit.

The NLO analytic terms are

$$p_H = \frac{1}{2(4\pi f_\pi)^2} [p_1(m_l, m_h) + p_2(m_q)] \quad (3.4)$$

$$p_1 = f_1(\Lambda_\chi) \left[\frac{11}{9}\mu(2m_l + m_h) + a^2 \left(\frac{3}{2}\bar{\Delta} + \frac{1}{3}\Delta_I \right) \right] \quad (3.5)$$

$$p_2 = f_2(\Lambda_\chi) \left[\frac{5}{3}\mu m_q + a^2 \left(\frac{3}{2}\bar{\Delta} - \frac{2}{3}\Delta_I \right) \right], \quad (3.6)$$

where $\bar{\Delta}$ is the weighted average of taste splittings. The $O(a^2)$ terms ensure that dependence upon the chiral logarithm scale, Λ_χ , in f_1 and f_2 cancels that of Δf_q .

Equation (3.2) with the addition of four NNLO analytic terms parameterizes our chiral extrapolations. We fit ϕ_{H_q} to determine the parameters. Constraints (value and width) for μ , Δ_ξ , f_π , δ'_A and δ'_V come from χ PT for lattice pions and kaons [8]. The coupling $g_{D^*D\pi}^2 = 0.35 \pm 0.14$ is likewise constrained by the CLEO measurement [9]. From heavy quark symmetry we expect $g_{B^*B\pi}^2 \approx g_{D^*D\pi}^2$. The remaining parameters Φ_H , f_1 and f_2 and the NNLO analytic parameters are determined in the fit.

In order to extrapolate to the physical results we set $\Delta_\xi = \delta'_{A,V} = 0$, $m_h \rightarrow m_s$ and $m_l \rightarrow (m_u + m_d)/2$. Then ϕ_{H_d} (ϕ_{H_s}) is found in the limit $m_q \rightarrow m_d$ (m_s).

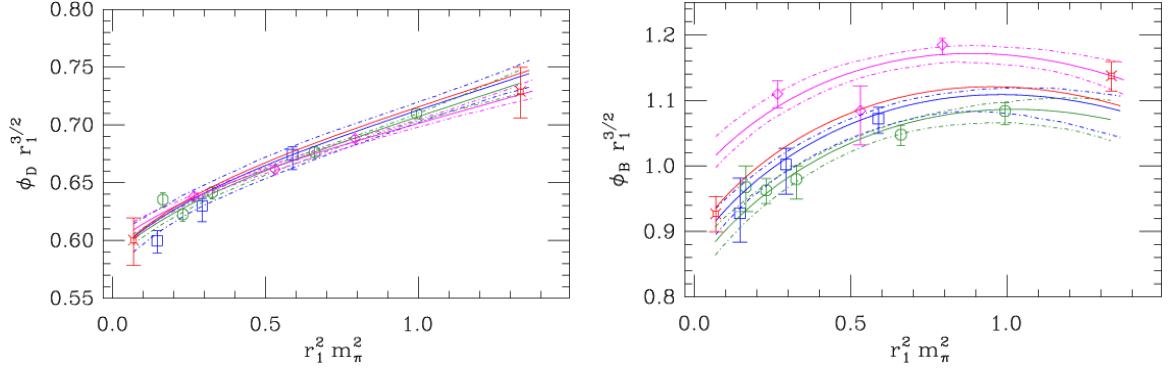


Figure 1: Chiral fits for the D (left) and B (right) mesons. Each fit is viewed along the direction in which $m_q = m_l$. Each fit is shown as a set of solid curves with the 68% confidence limits denoted by broken curves. Only statistical errors are shown. The $a = 0.09$ fm curve and data points are shown in blue, 0.12 fm in green and 0.15 fm in magenta. The $a^2 \rightarrow 0$ extrapolation curve and the $\phi_{H_{d,s}}$ points at physical values of m_u , m_d and m_s are shown in red. The statistical errors on the D and B physical points are of comparable size.

4. The Fit and Extrapolation for D and B

We determine both ϕ_{D^+} and ϕ_{D_s} from a single fit of ϕ_{D_q} simulation results using the expression in Eqn. (3.2), adding the four NNLO analytic terms and allowing for an explicit $O(a^2)$ term. We combine simulation results from 11 gauge ensembles at lattice spacings of $a = 0.09, 0.12$ and 0.15 fm in the fit. A total of 116 points are included in the fit. A bootstrap procedure propagates errors and correlations among the simulated results through to the statistical errors on our results. An analogous fit procedure for the B meson simulation results yields ϕ_{B_d} and ϕ_{B_s} .

The D and B meson fits combining the three lattice spacings are shown in Figs. 1 and 2. Figure 1 shows each fit and the data points along the $m_q = m_l$ direction while Fig. 2 shows the valence mass dependence of the fit at fixed values of the sea quark mass. All of the fit points are visible in Fig. 2 while only the subset of points with $m_q = m_l$ is visible in Fig. 1.

Figure 1 shows the D system on the left and the B system on the right. In each plot, the solid blue, green and magenta curves are the fit to the lattice data for lattice spacings 0.09, 0.12 and 0.15 respectively. These curves include the a^2 effects described by the chiral fit function. The 68% confidence limits for each curve are indicated by dotted contours of the corresponding color.

In Fig. 2 we show the valence mass dependence the D and B systems. In each plot the D system (blue points and curves) is shown together with B system (green points and curves). Each plot in the figure corresponds to a single combination of lattice spacing and m_l from Table 1. Together, the points represent all of the simulation results for ϕ_{H_q} used in this study. The fit curves include the a^2 effects described by the chiral fit function. Each curve is shown with its 68% confidence contours. The expression in Eqn. (3.2) predicts a divergent logarithmic rise as $m_q \rightarrow 0$ with m_l fixed. Our fits detect these logarithms even though taste breaking effects obscure them, so they are not immediately obvious in the plots.

The extrapolation, $a \rightarrow 0$, $m_h \rightarrow m_s$ and $m_l = m_q$ is shown in Fig. 1 as a solid red curve for each of the D and B systems. Our result for ϕ_{D^+} (ϕ_{B_d}) is found from the extrapolation by setting $m_l = \hat{m} = (m_u + m_d)/2$ and $m_q = m_d$. Likewise, ϕ_{D_d} (ϕ_{B_s}) is found by setting $m_q = m_s$. The physical

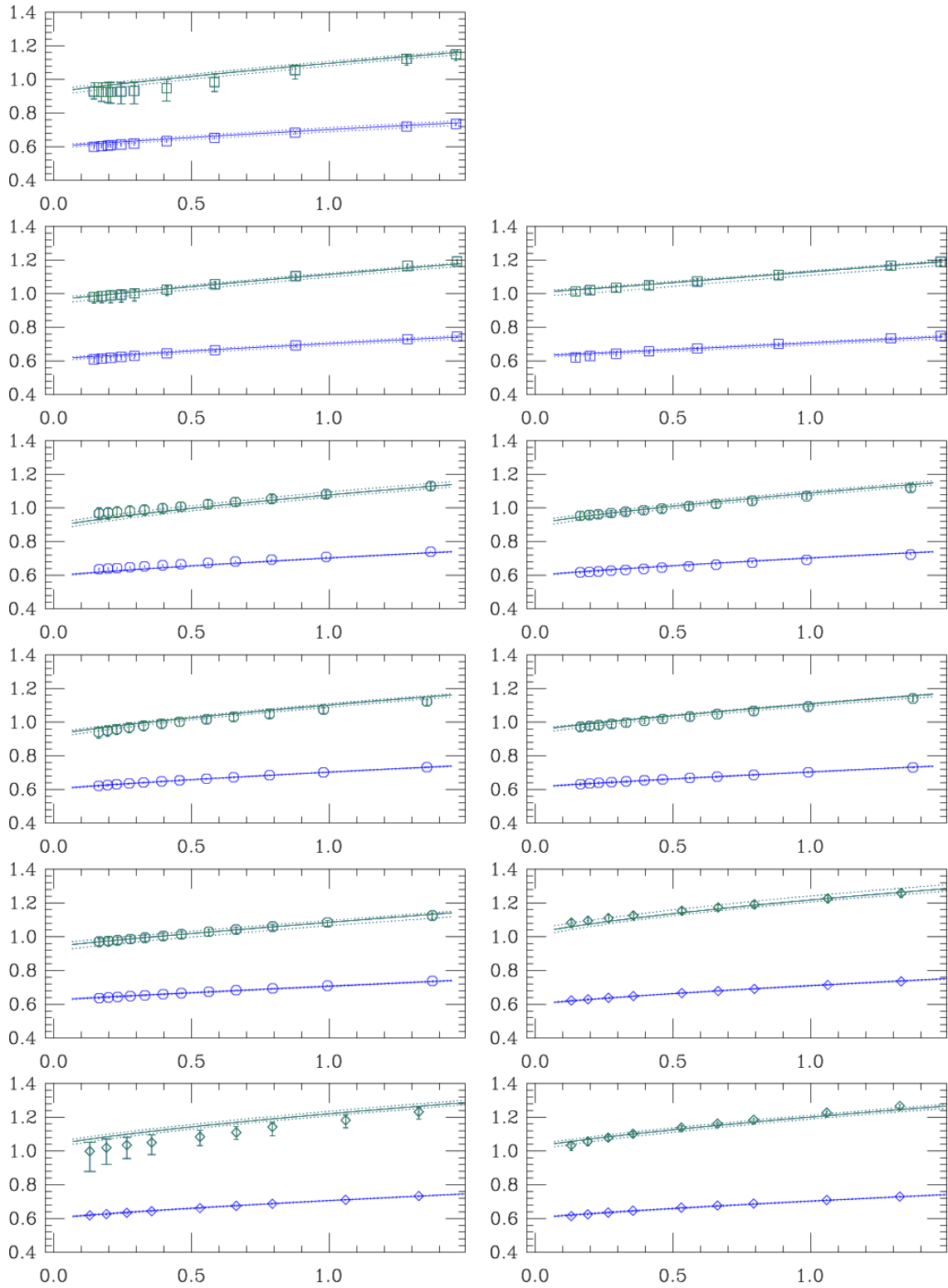


Figure 2: The m_q dependence of the single D fit (in blue) and the single B fit (in green) at fixed m_l . The figures ordered from left-to-right and top-to-bottom, have am_l equal to 0.0031, 0.0062, 0.0124 ($a = 0.09$ fm), 0.005, 0.007, 0.01, 0.02, 0.03 (0.12 fm), 0.0097, 0.0194 and 0.029 (0.15 fm) respectively. On the y-axis is $r_1^{3/2} \phi_{Hq}$ and on the x-axis is $r_1^2 m_\pi^2$. All 116 points in each fit are shown. The $\chi^2 = 98.6$ for the D fit and 48.5 for the B fit.

quantity	value	
ϕ_{D_s}	0.356(11)	GeV ^{3/2}
ϕ_{D_d}	0.293(11)	GeV ^{3/2}
$R_{D_{d/s}}$	0.824(8)	
ϕ_{B_s}	0.556(12)	GeV ^{3/2}
ϕ_{B_d}	0.453(13)	GeV ^{3/2}
$R_{B_{d/s}}$	0.815(15)	

Table 2: The main results of this preliminary study.

results are indicated with the red burst symbols. Since these points are projected into the $m_q = m_l$ plane of each figure, the central values do not lie on the red curve. The statistical errors for the physical ϕ_{H_q} values are shown in each figure. We find statistical errors comparable in magnitude for the physical ϕ_{D_q} and ϕ_{B_q} results.

5. Results and Outlook

Our preliminary results for the physical ϕ_{H_q} values and ratios with their statistical errors are in Table 2. We tabulate the major sources of uncertainty in Table 3. We omit listing uncertainties arising from terms of order $1/m_H$ in the chiral extrapolations since adding such terms changes the final results by less than the statistical errors. Such effects are still under investigation. Uncertainties from the input parameters r_1 and the light quark masses are found by propagating the uncertainties found in the MILC f_π and f_K determinations [5]. We estimate a 3.8% uncertainty in the bare charm mass and a 6.8% uncertainty in the bare bottom mass from variations in tuning procedures for the 0.09 fm lattice. Using simulation results for two heavy-quark masses near both charm and bottom, we estimate the uncertainties in ϕ_{H_q} . The uncertainties in Z_V^{ff} are statistical. Errors from unknown higher orders in ρ_{A_4} are estimated by considering higher orders effects to be as large as the 1-loop terms. Heavy quark discretization effects are estimated by power counting arguments. The dominant uncertainty in ϕ_{H_q} comes from effects of order $\alpha_s \Lambda a \times h(am)$ and $a^2 \Lambda^2$, where $h(am)$ is some mild function of the heavy quark mass. The uncertainties in the ratios are smaller by a factor of m_s/Λ . Light quark discretization effects are estimated by varying the extrapolation procedure. Finite volume effects are estimated by comparing theories at finite volume to the continuum.

From Table 2 and the experimental D^+ , D_s , B^0 and B_s masses we compute the decay constants:

$$f_{D_s} = 254 \pm 8 \pm 11 \text{ MeV} \quad (5.1)$$

$$f_{D^+} = 215 \pm 8 \pm 11 \text{ MeV} \quad (5.2)$$

$$f_{B_s} = 240 \pm 5 \pm 11 \text{ MeV} \quad (5.3)$$

$$f_{B_d} = 197 \pm 6 \pm 12 \text{ MeV} \quad (5.4)$$

where each of the first errors is statistical. The second error is the systematic error combined in quadrature from Table 3.

We also consider ratios of B to D decay constants where statistical and systematic errors are expected to be reduced due to cancellations. Statistical errors in the ratios are from a bootstrap

source	ϕ_{D_s}	ϕ_{D_d}	$R_{d/s}$	ϕ_{B_s}	ϕ_{B_d}	$R_{d/s}$
statistics	3.1	3.8	1.0	2.1	3.1	1.8
inputs r_1, m_s, m_d and m_u	1.4	2.0	0.5	3.1	3.8	0.6
input m_c or m_b	2.7	2.7	<0.1	1.1	1.1	<0.1
Z_V^{QQ} and Z_V^{qq}	1.4	1.4	0	1.4	1.4	0
higher-order ρ_{A_4}	0.3	0.3	<0.2	1.3	1.1	<0.2
heavy quark discretization	2.7	2.7	0.3	1.9	1.9	0.2
light quark discretization	1.0	2.7	1.8	2.0	3.8	1.8
finite volume	0.2	0.6	0.6	0.2	0.6	0.6
total systematic	4.4	5.3	2.0	4.7	6.1	2.0

Table 3: The error budget for the decay constants and their ratios. Uncertainties are quoted as a percentage. The total combines systematic errors in quadrature.

procedure in order to preserve statistical correlations.

$$f_{D^+}/f_{D_s} = 0.845 \pm 0.008 \pm 0.017 \quad (5.5)$$

$$f_{B_d}/f_{B_s} = 0.821 \pm 0.015 \pm 0.017 \quad (5.6)$$

$$f_{B_d}/f_{D^+} = 0.919 \pm 0.051 \pm 0.056 \quad (5.7)$$

$$f_{B_s}/f_{D_s} = 0.945 \pm 0.043 \pm 0.043 \quad (5.8)$$

The overall systematic errors for the first two ratios come from Table 3. Systematic errors for the last two ratios also come from combining errors in quadrature. These errors may be overestimates since we have not studied possible correlations at present.

We will extend this study to include a lattice spacing of $a = 0.06$ fm. We will improve statistics at $a = 0.09$ and 0.12 fm and add another ensemble (sea quark mass combination) at 0.09 fm. A finer lattice spacing, more sea quark combinations and better statistics will help control light- and heavy-quark discretization effects and improve statistical errors. The new gauge configurations will be used by MILC to refine r_1 and the light quark masses inputs used in this study.

References

- [1] C. Aubin *et al.*, Phys. Rev. Lett. **95**, 122002 (2005) [arXiv:hep-lat/0506030].
- [2] M. Artuso *et al.* [CLEO Collaboration], Phys. Rev. Lett. **95**, 251801 (2005) [arXiv:hep-ex/0508057].
- [3] R. T. Evans, E. Gamiz, A. X. El-Khadra and M. Di Pierro, arXiv:0710.2880 [hep-lat].
- [4] C. Aubin *et al.*, Phys. Rev. D **70**, 094505 (2004) [arXiv:hep-lat/0402030].
- [5] C. Bernard *et al.* [MILC Collaboration], PoS **LAT2005**, 025 (2006) [arXiv:hep-lat/0509137].
- [6] A. X. El-Khadra, E. Gamiz, A. S. Kronfeld and M. A. Nobes, arXiv:0710.1437 [hep-lat].
- [7] C. Aubin and C. Bernard, Phys. Rev. D **73**, 014515 (2006) [arXiv:hep-lat/0510088].
- [8] C. Aubin *et al.* [MILC Collaboration], Phys. Rev. D **70**, 114501 (2004) [arXiv:hep-lat/0407028].
- [9] A. Anastassov *et al.* [CLEO Collaboration], Phys. Rev. D **65**, 032003 (2002) [arXiv:hep-ex/0108043].